Prediction of high Reynolds number flow over a circular cylinder using LES with wall modeling

By Meng Wang, Pietro Catalano †, AND Gianluca Iaccarino

1. Motivation and objectives

The objective of this work is to assess the viability and accuracy of large-eddy simulation (LES) with wall modeling for high Reynolds number complex wall-bounded flows. It is well known that the conventional LES is extremely expensive at high Reynolds numbers due to the need to resolve the small but dynamically-important near-wall flow structures. As a practical alternative, LES can be coupled with a wall model which models these near-wall effects and provides the LES with a set of approximate boundary conditions, often in the form of wall shear stress (Cabot & Moin 2000).

In recent years, wall models based on turbulent boundary layer (TBL) equations and their simplified forms (Balaras, Benocci & Piomelli 1996; Cabot & Moin 2000) have received much attention. These models, used with a Reynolds-averaged Navier-Stokes (RANS) type of eddy viscosity, have shown promise for complex-flow predictions. For instance, Wang & Moin (2001) employed this approach to simulate the flow past the asymmetric trailing edge of an airfoil at chord Reynolds number of 2.15×10^6, and obtained very good agreement with solutions from the full LES (Wang & Moin 2000) at a small fraction of the computational cost.

The flow around a circular cylinder represents a canonical problem for validating new approaches in computational fluid dynamics. It is therefore reasonable or even necessary to subject the hybrid LES/wall-modeling methodology to the same "grand challenge". To take the best advantage of wall modeling, we concentrate on the super-critical flow regime in which the boundary layer on the cylinder becomes turbulent prior to separation. This is, to our knowledge, the first such attempt using LES, although a related method known as detached-eddy simulation (DES), in which the entire attached boundary layer is modeled, has been tested in this type of flow (Travin *et al.* 1999). Breuer (2000) recently conducted an LES study at a high sub-critical Reynolds number of $Re_D = 1.4 \times 10^5$, and showed fairly good comparison with experimental data in the near wake. In the present work, three simulations, at $Re_D = 5 \times 10^5$, 1×10^6, and 2×10^6, have been performed. Preliminary results and comparisons with experimental data are summarized in this article.

2. Numerical method and procedure

The same LES code and wall model implementation as used by Wang & Moin (2001) are used for the present calculations. The energy-conservative numerical scheme is of hybrid finite-difference/spectral type, written for a C-mesh (Mittal & Moin 1997). The time advancement is achieved by the fractional-step method, in combination with the Crank-Nicolson method for viscous terms and third-order Runge-Kutta scheme for convective terms. A multi-grid iterative procedure is used to solve the Poisson equation for

† Centro Italiano Ricerche Aerospaziali (CIRA), Italy

pressure. The subgrid-scale stress (SGS) tensor is modeled using the dynamic SGS model (Germano *et al.* 1991; Lilly 1992).

The computational domain has a spanwise size of $2D$ (D = cylinder diameter), over which the flow is assumed periodic and 48 grid points are distributed uniformly. In the planes perpendicular to the span, 401×120 grid points are used in the C-mesh, extending approximately $22D$ upstream of the cylinder, $17D$ downstream of the cylinder, and $24D$ into the far-field. Potential-flow solutions are imposed as boundary conditions in the far-field, and convective boundary conditions are used at the outflow boundary. Running at a maximum CFL number of 1.5, the non-dimensional time step $\Delta t U_\infty / D$ typically varies between 0.0030 and 0.0045. To obtain the results presented here, the simulations have advanced at least 150 dimensionless time units. The statistics are collected over the last 75 or so time units.

Approximate boundary conditions on the cylinder surface are imposed in terms of wall shear stress estimated from a wall model of the form

$$\frac{\partial}{\partial x_2}\left(\nu + \nu_t\right)\frac{\partial u_i}{\partial x_2} = \frac{1}{\rho}\frac{\partial p}{\partial x_i}, \qquad i = 1, 3 \tag{2.1}$$

This is a simpler variant of the TBL equation model (Cabot & Moin 2000) which allows for easier implementation and lower computational cost. Although Wang & Moin (2001) have shown that the full TBL equations (with dynamically adjusted ν_t) give better results in their trailing-edge flow, the discrepancy may be partly related to a surface curvature discontinuity which is absent from the cylinder surface. Since the pressure is taken from the LES at the edge of the wall layer, Eq. (2.1) can be integrated to the wall to obtain an algebraic model for the wall shear stress components (Wang 1999)

$$\tau_{wi} = \frac{\rho}{\int_0^\delta \frac{dy}{\nu + \nu_t}}\left\{u_{\delta_i} - \frac{1}{\rho}\frac{\partial p}{\partial x_i}\int_0^\delta \frac{y\,dy}{\nu + \nu_t}\right\}, \tag{2.2}$$

where $u_{\delta i}$ denotes the tangential velocity components from LES at the first off-wall velocity nodes, at distance δ from the wall. In attached flows these nodes are generally placed within the lower edge of the logarithmic layer. In the present flow, however, δ^+ (in wall units) is found to vary from 0 to 100 depending on the local skin friction. The eddy viscosity is modeled by a damped mixing-length model: $\nu_t/\nu = \kappa y_w^+ \left(1 - e^{-y_w^+/A}\right)^2$, where $y_w^+ = y_w u_\tau / \nu$ is the distance to the wall in wall units, $\kappa = 0.4$, and $A = 19$.

3. Results and discussion

In Fig. 1, the contours of the vorticity magnitude at a given time instant and spanwise plane are plotted for $Re_D = 10^6$. Large coherent structures are visible in the wake, but they are not as well organized and periodic as in typical Kármán streets at lower (sub-critical) and higher (post-critical) Reynolds numbers. Compared to flows at lower Reynolds number (*e.g.* Kravchenko & Moin 2000; Breuer 2000), the boundary-layer separation is much delayed and the wake is narrower, resulting in a much smaller drag coefficient. Note that the rather thick layer seen along the cylinder surface consists mostly of vorticity contours of small magnitude. These levels are necessary for visualizing the wake structure, but are not representative of the boundary-layer thickness. The true boundary layer, with strong vorticity, is extremely thin in the attached region.

A comparison with two sets of experimental data of the mean pressure distribution

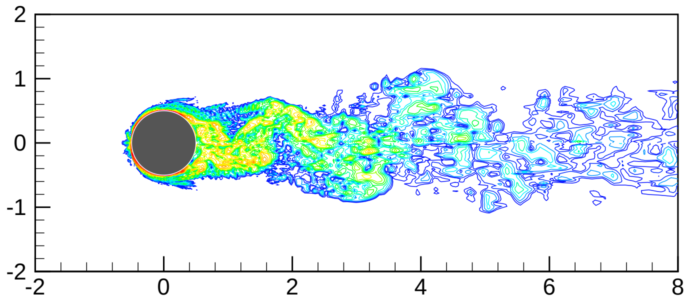

FIGURE 1. Instantaneous vorticity magnitude at a given spanwise cut for flow over a circular cylinder at $Re_D = 10^6$. 25 contour levels from $\omega D/U_\infty = 1$ to $\omega D/U_\infty = 575$ (exponential distribution) are plotted.

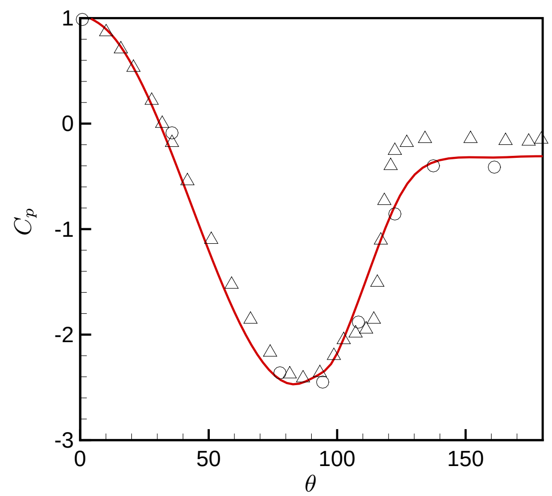

FIGURE 2. Mean pressure distribution on the circular cylinder. ——— Present LES at $Re_D = 10^6$; ○ Experiment of Warschauer & Leene (1971) at $Re_D = 1.26 \times 10^6$ (spanwise averaged); △ Experiment of Flachsbart (in Zdravkovich 1997) at $Re_D = 6.7 \times 10^5$.

on the cylinder surface is depicted in Fig. 2. Very good agreement is observed between the LES at $Re_D = 10^6$ and the experiment of Warschauer & Leene (1971) which was performed at $Re_D = 1.26\times10^6$. The original C_p data of Warschauer & Leene exhibit some spanwise variations; for the purpose of comparison the average value is plotted. Relative to the measurements of Flachsbart (see Zdravkovich 1997) at $Re_D = 6.7 \times 10^5$, the LES C_p shows smaller values in the base region. Note that Flachsbart's data contain a kink near $\theta = 110^o$, indicating the presence of a separation bubble. This type of separation bubble is characteristic of the critical regime, and is difficult to reproduce experimentally or numerically due to sensitivity to disturbances.

In Table 1, we compare the mean drag coefficient, the base pressure coefficient, and the Strouhal number from the LES at $Re_D = 10^6$ with the experimental values. The agreement with the measurements of Shih *et al.* (1993) is reasonably good. The LES somewhat overpredicts the drag coefficient compared with Shih *et al.* (1993), but underpredicts it relative to Achenbach (1968) (cf. Fig. 3). The Strouhal number of 0.22 from

	C_D	$-C_{p,base}$	St
LES	0.31	0.32	0.28
Exp. (Shih *et al.* 1993)	0.24	0.33	0.22
Exp. (Others, see Zdravkovich 1997)	0.17-0.40	–	0.18-0.50

Table 1. Drag, base pressure coefficient and Strouhal number for the flow around a circular cylinder at a Reynolds number of 10^6.

Shih *et al.* is for a rough-surface cylinder; no coherent vortex shedding was observed for smooth cylinders at Re_D larger than 4×10^5. Indeed, it is generally accepted that periodic vortex shedding does not exist in the super-critical regime of flow over a smooth cylinder (Zdravkovich 1997). From our simulation, a broad spectral peak of the unsteady lift centered at $St \approx 0.28$ is found. It can be argued that although the LES is performed for a smooth cylinder, the discretization of the cylinder surface and the numerical errors due to under-resolution may act as equivalent surface roughness, causing the flow field to acquire some rough-cylinder characteristics. The flow at high Reynolds number is very sensitive to surface roughness and to the level of free-stream turbulence, which contribute to the wide scatter of C_D and St among various experiments in the literature (Zdravkovich 1997), listed at the bottom of Table 1. Other factors causing the data scatter include wind-tunnel blockage and end-plate effects. Our simulation results fall easily within the experimental range. Generally speaking, there is a lack of detailed experimental data at super-critical Reynolds numbers. In particular, velocity and Reynolds-stress profile measurements are non-existent, making a more detailed comparison impossible.

To assess the robustness of the computational method, we have performed simulations at $Re_D = 5 \times 10^5$ and 2×10^6, in addition to the initial attempt at $Re_D = 1 \times 10^6$. The predicted mean drag coefficients are plotted in Fig. 3 along with the drag curve of Achenbach (1968). While the simulations predict C_D rather well at the two lower Reynolds numbers, the discrepancy becomes large at $Re_D = 2 \times 10^6$. More significantly, the LES solutions show relative insensitivity to the Reynolds number, in contrast to the experimental data which exhibit an increase in C_D with Reynolds number after the drag crisis. Similar Reynolds-number insensitivity has been observed for the other quantities shown previously. Poor grid resolution, which becomes increasingly severe as the Reynolds number increases, is the primary suspect.

Finally, the skin-friction coefficients predicted by the wall model in the LES calculations are plotted in Fig. 4 against the experimental data of Achenbach (1968) at $Re_D = 3.6 \times 10^6$. The levels are very different on the front half of the cylinder, but are in reasonable agreement on the back half. The boundary-layer separation and the recirculation region are captured rather well by the LES, indicating that they are not strongly affected by the upstream errors. The different Reynolds numbers in the LES and the experiment can account for only a small fraction of the discrepancy. Note that our computed C_f values are comparable to those reported by Travin *et al.* (2000) using DES. Travin *et al.* attribute the overprediction of C_f before separation to the largely-laminar boundary layer in the experiment, which has not been modeled adequately in either simulation. Grid resolution is another potential culprit in the present work. In addition, an overprediction of the skin

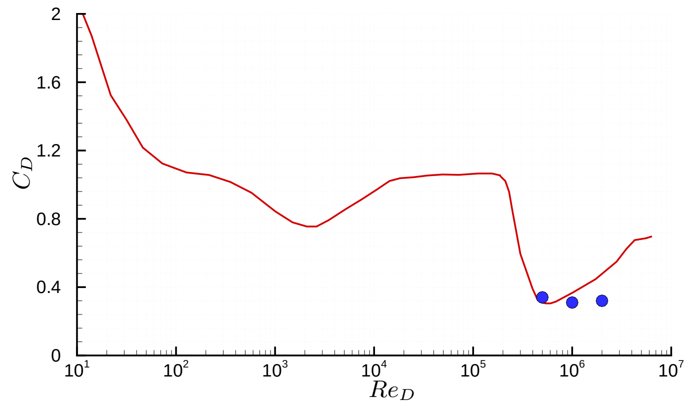

FIGURE 3. Drag coefficient as a function of Reynolds number. ——— Achenbach (1968); • Present LES.

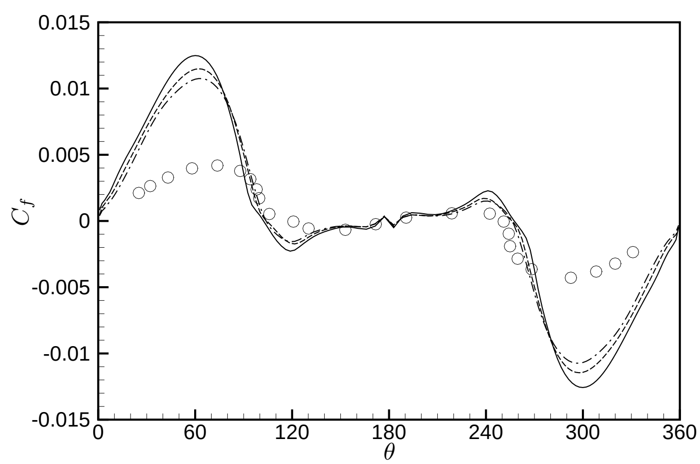

FIGURE 4. Skin friction distribution on the cylinder from LES: ——— $Re_D = 5 \times 10^5$; - - - - $Re_D = 1 \times 10^6$; —·— $Re_D = 2 \times 10^6$. ∘ Experiment of Achenbach (1968) at $Re_D = 3.6 \times 10^6$.

friction by the present wall model has also been observed by Wang & Moin (2001) in the acceleration region of the trailing-edge flow, suggesting that this simplified model may have difficulty with strong favorable pressure gradients. If this proves to be a major factor, the more general TBL equation model should provide a better alternative.

4. Concluding remarks

A bold numerical experiment has been carried out to compute the flow around a circular cylinder at supercritical Reynolds numbers using LES. The simulation is made possible by the use of a wall-layer model which alleviates the near-wall grid resolution requirements. Preliminary results are promising in the sense that they correctly predict the delayed boundary-layer separation and reduced drag coefficients consistent with measurements after the drag crisis. In quantitative terms, the mean pressure distributions and overall drag coefficients are predicted reasonably well at $Re_D = 5 \times 10^5$ and 10^6. However, the computational solutions are inaccurate at higher Reynolds numbers, and the Reynolds-number dependence of the drag coefficient is not captured.

It must be emphasized that the results presented here are very preliminary. The grid used near the cylinder surface, particularly before separation, is quite coarse judged by the need to resolve the outer boundary-layer scales. The effect of the wall model under coarse grid resolution and in the laminar boundary layer is not clear. Evidently, a more systematic investigation is needed to separate the grid resolution and wall modeling effects, and to fully validate the numerical methodology in this challenging flow.

REFERENCES

Achenbach, E. 1968 Distribution of local pressure and skin friction around a circular cylinder in cross-flow up to $Re = 5 \times 10^6$. *J. Fluid Mech.* **34**, 625-639.

Balaras, E., Benocci, C. & Piomelli, U. 1996 Two-layer approximate boundary conditions for large-eddy simulation. *AIAA J.* **34**, 1111-1119.

Breuer, M. 2000 A challenging test case for large eddy simulation: high Reynolds number circular cylinder flow. *Int. J. Heat Fluid Flow* **21**, 648-654.

Cabot, W. & Moin, P. 2000 Approximate wall boundary conditions in the large-eddy simulation of high Reynolds number flow. *Flow Turb. Combust.* **63**, 269-291.

Germano, M., Piomelli, U., Moin, P. & Cabot, W. H. 1991 A dynamic subgrid-scale eddy viscosity model. *Phys. Fluids A* **3**, 1760-1765.

Kravchenko, A.G. & Moin P. 2000 Numerical studies of flow over a circular cylinder at $Re_D = 3900$. *Phys. Fluids* **12**, 403-417.

Lilly D. K. 1992 A proposed modification of the Germano subgrid scale closure method. *Phys. Fluids A* **4**, 633-635.

Mittal, R. & Moin, P. 1997 Suitability of upwind-biased finite difference schemes for large-eddy simulation of turbulence flows. *AIAA J.* **35**, 1415-1417.

Travin, A., Shur, M., Strelets, M. & Spalart, P. 1999 Detached-eddy simulations past a circular cylinder. *Flow Turb. Combust.* **63**, 269-291.

Shih, W. C. L., Wang, C., Coles, D. & Roshko, A. 1993 Experiments on flow past rough circular cylinders at large Reynolds numbers. *J. Wind Engg and Industrial Aerodynamics* **49**, 351-368.

Wang, M. 1999 LES with wall models for trailing-edge aeroacoustics. *Annual Research Briefs*, Center for Turbulence Research, NASA Ames/Stanford Univ. 355-364.

Wang, M. & Moin, P. 2000 Computation of trailing-edge flow and noise using large-eddy simulation. *AIAA J.* **38**, 2201-2209.

Wang, M. & Moin, P. 2001 Wall modeling in LES of trailing-edge flow. *Proceedings of the Second International Symposium on Turbulence and Shear Flow Phenomena*, Stockholm, Sweden, **II**, 165-170.

Warschauer, K. A. & Leene, J. A. 1971 Experiments on mean and fluctuating pressures of circular cylinders at cross flow at very high Reynolds numbers. *Proc. Int. Conf. on Wind Effects on Buildings and Structures*, Saikon, Tokyo, 305-315 (see also Zdravkovich 1997).

Zdravkovich, M. M. 1997 *Flow Around Circular Cylinders. Vol. 1: Fundamentals.* Oxford University Press, Chap. 6.